Soliton evolution and associated sonic horizon formation dynamics in two-dimensional Bose-Einstein condensate with quintic-order nonlinearity

Soliton evolution and associated sonic horizon formation dynamics in two-dimensional Bose–Einstein condensate with quintic-order nonlinearity

Cite as: Chaos **31**, 023105 (2021); https://doi.org/10.1063/5.0031741
Submitted: 08 October 2020 . Accepted: 11 January 2021 . Published Online: 01 February 2021

Ying Wang, Yujie Chen, Jun Dai, Li Zhao, Wen Wen, and Wei Wang

Soliton evolution and associated sonic horizon formation dynamics in two-dimensional Bose–Einstein condensate with quintic-order nonlinearity

Cite as: Chaos **31**, 023105 (2021); doi: 10.1063/5.0031741
Submitted: 8 October 2020 · Accepted: 11 January 2021 ·
Published Online: 1 February 2021

View Online Export Citation CrossMark

Ying Wang,[1,2,a)] Yujie Chen,[1,2] Jun Dai,[1,2,b)] Li Zhao,[3] Wen Wen,[4] and Wei Wang[2,5,c)]

AFFILIATIONS

[1]School of Science, Jiangsu University of Science and Technology, Zhenjiang 212100, China
[2]Laboratory of Advanced Optics, Jiangsu University of Science and Technology, Zhenjiang 212100, China
[3]School of Materials Science and Engineering, Jiangsu University of Science and Technology, Zhenjiang 212100, China
[4]College of Science, Hohai University, Nanjing, Jiangsu 210098, China
[5]Institute of Photonics and Quantum Sciences, School of Engineering and Physical Sciences, Heriot-Watt University, Edinburgh EH14 4AS, United Kingdom

[a)]**Author to whom correspondence should be addressed:** wangying@just.edu.cn
[b)]**Electronic address:** daijun@just.edu.cn
[c)]**Electronic address:** w.wang@hw.ac.uk

ABSTRACT

This study explored the two-dimensional Bose–Einstein condensate with an inter-particle nonlinear interaction up to quintic order. Based on the two-dimensional Gross–Pitaevskii equation model with quintic-order nonlinearity, we first derived the bright soliton solution for the system based on the self-similar approach and the modified variational method. We identified that the kinematic quantities derived from the two methods agreed very well. The two-dimensional sonic horizon formation dynamics was then calculated based on the bright soliton solution that was obtained. The periodic formation and evolution patterns of the two-dimensional sonic horizon were quantitatively analyzed and pictorially illustrated. The results can be used to guide sonic black hole related phenomenon observations in a two-dimensional Bose–Einstein condensate with quintic-order nonlinearity.

Black hole is originally the fascinating phenomenon in astrophysics for its peculiar features including the trapping of everything including light within the event horizon and predicted Hawking radiation. It is discovered that many intriguing features of black hole like formation of event horizon (boundary of trapping region) can be studied by its acoustic analog in ultracold atomic system-sonic black hole, which has the additional merits of easy manipulation, repeatability of occurrence, and low cost. Our work will investigate the sonic horizon formation of a sonic black hole in a two-dimensional Bose–Einstein condensate, where the evolution of sonic horizon, which is stabilized by an appropriate higher-order nonlinear interaction, can be clearly visualized from our theoretical study and will pave the way for an experimental observation of a sonic black hole study in a two-dimensional Bose–Einstein condensate.

I. INTRODUCTION

Nonlinear phenomena are a fascinating subject in the realms of physical science. This fascination is partially attributed to understanding soliton behavior. This is an intriguing nonlinear phenomenon that happens when the dispersion and a nonlinear interaction effects balance in certain existence mediums such as an optical fiber or a Bose–Einstein condensate (BEC).[1–4] It is well known that a stable soliton exists in a one-dimensional system[5–8] modeled by a traditional nonlinear Schrödinger equation (NLSE) or a Gross–Pitaevskii equation (GPE)[9–20] with cubic nonlinearity. It has also been recently demonstrated in other studies that in higher-dimensional systems with higher-order nonlinear interactions, a stable soliton behavior can also exist, such as a stable optical soliton traveling in a hollow optical cable filled with cold atomic gas.[21] Also arising from the flexible and relatively easy modulation, ultracold atomic systems can act as an ideal platform to study the analog black hole–sonic black hole. This is an intriguing nonlinear phenomenon arising from the manipulation of inter-particle nonlinear interactions and the evolution of soliton or soliton-like behavior of the system. The basis of a sonic black hole comes from the identification of quantum flow and the system excitation with spacetime and spacetime fields in astrophysics, respectively, as pointed out by Unruh.[22] There are high costs and unrepeatable occurrences of a black hole in astrophysics. However, ultracold atomic settings such as BECs, where sonic black hole formations exist, can be used to study black hole related problems such as Hawking radiation with flexible manipulation of such a system setting,[23] with less cost or associated problems.

While there are relatively many works focusing on the one-dimensional systems modeled by one-dimensional GPE[24,25] with leading order nonlinearity, actual physical systems are usually higher-dimensional and call for the study of typical modes such as solitons when a higher-order nonlinear interaction is incorporated. In this work, we explored a two-dimensional BEC based on a two-dimensional GPE with quintic-order nonlinearity, which corresponds to the system with strong harmonic confining potential in the longitudinal z direction. With the investigation of higher-dimensional soliton-like behavior,[12–16] we first derived the two-dimensional bright soliton solution of the system based on self-similar[12,13] and modified variational methods.[26,27] This is where our analysis reached matched kinematic quantities from two different methods, and it demonstrated the applicability of the theoretical treatment made in the course of our analysis. Utilizing the system bright soliton wave function and system flow velocity derived from the two methods, we calculated the two-dimensional sonic horizon formation criteria formula and then derived the sonic horizon equation. The sonic horizon boundary, which separates the systems' ultrasonic and subsonic flow regions, is shown in a three-dimensional plot of the system sound and the flow velocity distribution. Also, the periodic evolution patterns of the two-dimensional sonic horizon oscillates between its disappearance, line-shape appearance, and closed ellipse-like curve. The analytical results obtained in this study can be used to guide two-dimensional sonic black hole phenomenon observations in two-dimensional quantum systems with quintic-order nonlinearity.

This study is organized as follows. Section II presents the bright soliton results for one-dimensional BEC with quintic-order nonlinearity based on the corresponding one-dimensional GPE model. Sections III and IV derived the two-dimensional bright soliton solution for two-dimensional BEC with quintic-order nonlinearity based on two-dimensional GPE via a self-similar method and a modified variational method, respectively. Section V derived the two-dimensional sonic horizon formation and evolution dynamics, with the analytical results pictorially illustrated. Section VI provides concluding remarks regarding the obtained results of the study.

II. BRIGHT SOLITON IN ONE-DIMENSIONAL BEC MODELED WITH (1+1)-DIMENSIONAL GPE INCORPORATING QUINTIC-ORDER NONLINEARITY

Incorporating the typical quintic-order nonlinear interaction of one-dimensional (or quasi-one-dimensional) BEC, the 1D GPE model has the following form:

$$i\hbar\frac{\partial}{\partial t}\psi(x,t)+\frac{\hbar^2}{2m}\frac{\partial^2}{\partial x^2}\psi-kx^2\psi+(g_1|\psi|^2+g_2|\psi|^4)=0, \quad (1)$$

where $k=\frac{1}{2}m\Omega^2$ is the potential strength of the one-dimensional harmonic potential in the system. Items g_1, g_2 are cubic and quintic-order nonlinear strength coefficients, respectively, corresponding to two-body and three-body interactions between particles in the system. In prior work,[28] the typical analytical solitons of Eq. (1) is derived as follows:

$$\psi_{1D}=C_0^{1/2}\sqrt{\frac{1}{d^{\frac{1}{2}}\cosh[a_2^{\frac{1}{2}}(px+q(t))]+C_1}}, \quad (2)$$

where constants C_0, C_1, d, a_2, p and $q(t)=\chi(t)t$ are determined by the initial conditions and the t dependence of $\chi(t)=q(t)/t$ arises from the nonzero trapping strength k. The formulation of Eq. (2) for the case $k=0$ coincides in a functional form [same x and t dependence with $\chi(t)=\chi$, and the phase function is in the form of $Px+Wt=\Phi_2(t)x^2+\Phi_1(t)x+\Phi_0(t)=\Phi_1(t)x+\Phi_0(t)$ with $\Phi_2(t)=0$, $P=\Phi_1(t)$, and $W=\Phi_0(t)/t$ taking constant values, where $\Phi_2(t)$, $\Phi_1(t)$, and $\Phi_0(t)$ are defined in the work[28] just referenced] with that derived in prior work[29,30] (same quintic nonlinearity but with $k=0$).

It is not difficult to see that Eq. (2) is of a bright soliton type. We start from solution (2) to derive the two-dimensional sonic dynamics for the system. It is important to perform some stability analysis for solution (2). Suppose the small perturbation to the wave function (2) is $\tilde{\psi}$ so that the wave function is in the form

$$\psi(x,t)=[\psi_{1D}(x,t)+\tilde{\psi}(x,t)]e^{i\mu_0 t}, \quad (3)$$

where $\tilde{\psi}(x,t)=\tilde{U}(p_0(t)x+q_0(t))e^{i\mu(x,t)}$, $\mu(x,t)=\phi_2(t)x^2+\phi_1(t)x$ as defined in prior work.[28] Substituting the perturbed wave function (3) into Eq. (1) and with the proper choice of $\phi_2(t)$ and $\phi_1(t)$, the time derivative and the second order spatial derivative on $\mu(x,t)$ combined with the time derivative on $p_0(t)$ will eliminate the terms of $x^2\tilde{U}$ and $x\frac{\partial\tilde{U}}{\partial x}$ in the resultant equation for $\tilde{U}(x,t)$, which takes the following form [in natural units and make notations $\tau=q_0(t)$ as t, $p_0(t)x$ as x],

$$i\tilde{U}_t+\tilde{U}_{xx}-\mu_0\tilde{U}+[F(\psi_{1D}^2)+\psi_{1D}^2F'(\psi_{1D}^2)]\tilde{U}+\psi_{1D}^2F'(\psi_{1D}^2)\tilde{U}^*=0, \quad (4)$$

where $F(\psi_{1D}^2)=g_1|\psi_{1D}|^2+g_2|\psi_{1D}|^4$. Therefore, our stability analysis problem is reduced to the same category of problems shown in some prior work,[31] which studied various normal modes of Eq. (4) in the following form:

$$\tilde{U}_{mode}(x,t)=f(x)e^{\lambda t}+g^*(x)e^{\lambda^* t}. \quad (5)$$

As demonstrated in Ref. 31 (with stability analysis for parameters g_1 and g_2), the eigenvalue λ is pure imaginary; thus, the solution (2) is stable with an appropriate system setting (including g_1 and g_2) for Eq. (1) with quintic nonlinearity.

Next, we will investigate the dynamical soliton behavior of the two-dimensional system with a quintic-order nonlinear effect in two distinct ways. One is the self-similar method based on a one-dimensional soliton solution. Another method is the modified variational method based on a modified ansatz of the system wave function. A comparison of the typical soliton solutions was made by implementing these two methods, which can deepen our understanding of typical soliton behavior in two-dimensional BEC.

III. THE SOLITON DYNAMICAL BEHAVIOR OF TWO-DIMENSIONAL BEC WITH QUINTIC-ORDER NONLINEARITY BASED ON A SELF-SIMILAR METHOD

First, based on the bright solitary soliton of one-dimensional GPE, we used a self-similar method to obtain the bright soliton dynamics behavior of a two-dimensional BEC system with a quintic-order nonlinear effect. We start from the two-dimensional GPE equation with a quintic-order nonlinear effect ($m = \hbar = 1$),

$$\frac{i\partial}{\partial t}\psi = \left[-\left(\frac{\partial^2}{\partial x^2} + \frac{\partial^2}{\partial y^2}\right) + k(x^2+y^2) + g_1|\psi|^2 + g_2|\psi|^4\right]\psi. \tag{6}$$

In order to eliminate the integrable constraints generated in the process of applying the self-similar method, we introduce the parametric function $z(t)$ of time t into the transformation of coordinates of Eq. (6), which is as follows:

$$x' = z(t)x, \tag{7a}$$

$$y' = z(t)y, \tag{7b}$$

$$t' = \int z^2(t)dt. \tag{7c}$$

The corresponding wave function is transformed as follows:

$$\psi(x,y,t) = z(t)\exp\left[-\frac{i}{4}\frac{z_{t'}(t')}{z(t')}(x'^2+y'^2)\right]\varphi(x',y',t'), \tag{8}$$

where $z_{t'}(t') = \frac{dz(t')}{dt'}$. We change the notation of x', y', t' to x, y, t and substitute Eqs. (7) and (8) into Eq. (6) , and the equation for the wave function $\varphi(x,y,t)$ takes the following form:

$$i\frac{\partial\varphi}{\partial t} + \left(\frac{\partial^2}{\partial x^2} + \frac{\partial^2}{\partial y^2}\right)\varphi + [u_0(t)|\varphi|^2 + u_1(t)|\varphi|^4] + \rho(t)(x^2+y^2)\varphi = 0, \tag{9}$$

where x', y', t' have been denoted as x, y, t,

$$u_i(t) = g_i z^{2i+2}(t)(i = 0,1), \tag{10a}$$

$$\rho(t) = \frac{1}{4z^2(t)}\left\{4k(t) + \frac{z_t^2}{z^2(t)} - \left[\frac{z_t(t)}{z(t)}\right]_t\right\}. \tag{10b}$$

The (1+1)-dimensional self-similar GPE equation of the two-dimensional GPE with a quintic-order nonlinear interaction is

$$i\frac{\partial\phi}{\partial\tau} + \epsilon\frac{\partial^2\phi}{\partial\xi^2} + k'(t)\xi^2\phi + \delta_1|\phi|^2 + \delta_2|\phi|^4 = 0, \tag{11}$$

where $\phi = \phi(\xi,\tau)$, and the self-similar solution of Equation (6) is in the following form:

$$\varphi(x,y,t) = A(t)\phi[\xi(x,y,t),\tau(t)]\exp[ia(x,y,t)]. \tag{12}$$

$A(t), \xi(x,y,t), \tau(t)$, and $a(x,y,t)$ are to be determined in the following steps together with the parametric function $z(t)$, substituting Eq. (12) into Eq. (9), and the resulting equation is arranged into the form of Eq. (11). The following set of equations are obtained:

$$2u_0(t)A^2 - \delta_1\tau_t = 0, \tag{13a}$$

$$2u_1(t)A^4 - \delta_2\tau_t = 0, \tag{13b}$$

$$(\xi_x^2 + \xi_y^2) - \epsilon\tau_t = 0, \tag{13c}$$

$$\xi_t + 2(\xi_x a_x + \xi_y a_y) = 0, \tag{13d}$$

$$2A_t + 2A(a_{xx} + a_{yy}) = 0, \tag{13e}$$

$$a_t + a_x^2 + a_y^2 + a_z^2 - (\rho(t) + k'(t))(x^2+y^2) = 0. \tag{13f}$$

Equation (13) can be solved with the help of the parameter function $z(t)$ without additional integrable constraints. The specific solutions are as follows:

$$A(t) = \sqrt{\frac{2\delta_1}{\epsilon u_0}}G, \tag{14a}$$

$$\xi(x,y,t) = -4D_1\int G^2dt + G(x+y) + D_2, \tag{14b}$$

$$\tau(t) = \frac{2}{\epsilon}\int G^2dt + D_3, \tag{14c}$$

$$a(x,y,t) = \frac{u_{0t}(t)}{4u_0(t)}(x^2+y^2) + D_1G(x+y) - 2D_1^2\int G^2dt + D_4, \tag{14d}$$

where $G = \exp[-\int \frac{u_{0t}(t)}{u_0(t)}]$, $u_{0t}(t) = \frac{du_0(t)}{dt}$, D_1, D_2, D_3, D_4 are the integral constants. $u_0(t)$ and $\rho(t)$, which are determined by $z(t)$, satisfy the following equation:

$$\frac{1}{u_0(t)}\frac{d^2u_0(t)}{dt^2} - 4(\rho(t) + k'(t)) = 0, \tag{15}$$

where $u_0(t)$ and $\rho(t)$ are represented by Eq. (10a) and Eq. (10b). By substituting Eqs. (10a) and (10a) into Eq. (15), we get the following equation that $z(t)$ satisfies:

$$\frac{1}{z_t^2}\frac{d[z^2(t)]}{dt^2} - \frac{1}{z^2(t)}\left\{4[k(t)+k'(t)] + \frac{z_t^2}{z(t)^2} - \left[\frac{z_t(t)}{z(t)}\right]_t\right\} = 0. \tag{16}$$

Equation (16) has the following general solution:

$$z(t) = z_1\sin(2\Omega t) + z_2, \tag{17}$$

where z_1 and z_2 are the constants to be determined by the initial condition. We can see from Eqs. (12) and (14b) that $z(t)$ determines the magnitude of the system's flow speed. We will corroborate this quantitative result based on the variational approach in Sec. IV.

IV. THE SOLITON DYNAMICS OF TWO-DIMENSIONAL BEC WITH A QUINTIC-ORDER NONLINEAR INTERACTION BASED ON A MODIFIED VARIATIONAL METHOD

In order to further understand the behavior of a two-dimensional soliton solution obtained in Sec. III, we search for two-dimensional BEC soliton dynamical behavior by using the modified variational method based on GPE with quintic-order nonlinear interactions. We start with the Lagrangian density L of Eq. (6), which takes the following form:

$$L(x,y,t) = \psi^* \left[i\frac{\partial}{\partial t} + \frac{1}{2}\left(\frac{\partial^2}{\partial x^2} + \frac{\partial^2}{\partial y^2}\right) - k(x^2+y^2) - \frac{1}{2}g_1|\psi|^2 - \frac{1}{3}g_2|\psi|^4 \right]\psi. \tag{18}$$

We aim to find the single bright soliton solutions of two-dimensional BEC described in Eq. (6); then, we discuss the obtained ground state wave function and compared it with the two-dimensional bright soliton solutions obtained in Sec. III. For this purpose, the following ansatz for the wave function is adopted:

$$\psi(x,y,t) = \frac{C_1}{\nu(t)}\varphi_{1D}\left(\frac{b_1 x}{\nu(t)} + \frac{b_2 y}{\nu(t)}, t\right)\exp[-i\beta(t)(x^2+y^2)], \tag{19}$$

where C_1 is the normalization constant. Comparing with the traditional variational Gaussian ansatz function $\varphi(x,y) = \exp[-\frac{1}{2}(x^2+y^2)]$, the (1+1) dimensional ansatz function $\varphi_{1D}(x',t)$ in Eq. (19) takes the form of ψ_{1D} in Eq. (2). It is more precise and takes the following form:

$$\varphi_{1D}\left(\frac{1}{\nu(t)}(b_1x+b_2y), t\right) = C_0^{\frac{1}{2}}\sqrt{\frac{1}{d^{\frac{1}{2}}\cosh[a_2^{\frac{1}{2}}(b_1'x+b_2'y)+qt]+C}}, \tag{20}$$

where $b_1' = b_1/\nu(t)$, $b_2' = b_2/\nu(t)$. Substituting Eqs. (19) and (20) into Eq. (6) and eliminating the common factor $\exp[-i\beta(t)(x^2+y^2)]$ of each term of the equation, we obtain the imaginary part of Eq. (6) as follows:

$$\beta(t) = -\frac{1}{2}\frac{\dot{\nu}(t)}{\nu(t)}. \tag{21}$$

Also, $\nu(t)$ is solved by integrating the space coordinates x,y of $L(x,y,t)$ in $S = \int\int L(x,y,t)dxdydt$ and takes the Euler–Lagrangian equation for $\nu(t)$, which is as follows:

$$\ddot{\nu}(t) = \frac{d^2\nu(t)}{dt^2} = -\frac{\partial U(\nu)}{\partial \nu}, \tag{22}$$

where

$$U(\nu) = U_0(\nu) + U_1(\nu) + U_2(\nu), \tag{23a}$$

$$U_0(\nu) = k\nu^2 + \frac{C_2''}{2C_1''}\frac{1}{\nu^2}, \tag{23b}$$

$$U_1(\nu) = g_1\frac{C_3''}{C_1''}\frac{1}{\nu^2}, \tag{23c}$$

$$U_2(\nu) = g_2\frac{C_4''}{(C_1'')^2}\frac{1}{\nu^4}, \tag{23d}$$

$$C_1'' = \int_0^\infty \nu x'^2\varphi_{1D}^2(x')dx', \tag{23e}$$

$$C_2'' = \int_0^\infty \frac{d\varphi_{1D}^2}{dx'}dx', \tag{23f}$$

$$C_3'' = \int_0^\infty \varphi_{1D}^2 dx', C_4'' = \int_0^\infty \varphi_{1D}^4 dx'. \tag{23g}$$

When the intensity coefficients of the nonlinear interaction g_1 and g_2 are very small, we can make an approximation $U = U_0$, and Eq. (22) becomes

$$\ddot{\nu}(t) = -\frac{\partial U_0(\nu)}{\partial \nu}. \tag{24}$$

Equation (24) has the following analytical solution:

$$\nu(t)^2 = \nu_1 \sin\omega t + \nu_2, \tag{25}$$

where

$$\nu_1 = \sqrt{\left(\frac{\nu_0^2}{2} + \frac{1}{4k\nu_0^2}\right)^2 - \frac{C_2''}{4C_1''}}, \tag{26a}$$

$$\nu_2 = \frac{\nu_0^2}{2} + \frac{C_2''}{4C_1''\nu_0^2}, \tag{26b}$$

$$\omega = 2\Omega, \tag{26c}$$

where ν_0 is the initial expansion width determined by the initial conditions. It can be seen that the expansion width $\nu(t)$ of the two-dimensional bright soliton represented by the function $\varphi_{1D}(\frac{1}{\nu(t)}(b_1x+b_2y), t)$ oscillates periodically between the maximum $\sqrt{\nu_2+\nu_1}$ and the minimum $\sqrt{\nu_2-\nu_1}$.

Now, we perform some stability analysis of our analytical solution derived. The existence of stable [may be of dynamical stable periodic motion around the minimum ν-coordinate ν_m of the potential curve $U(\nu)$ shown in Fig. 1] $\nu(t)$ depends on the occurrence of ν_m of the potential curve shown in Fig. 1, which should locate within the system's spatial domain. Also, according to Eq. (23), the "total energy" is $E = \frac{1}{2}m\dot{\nu}^2(t) + U(\nu(t)) = E_0$, which is integral constant (sum of variable "kinetic energy" and variable "potential energy") that is determined by the initial condition. Evolution of $\nu(t)$ will proceed in a stable manner around the minimum ν_m with a significant depth. We can see from Fig. 1 that the existence of the stability range has qualitative dependence on the zeroth order part (U_0) of $U(\nu)$; typical (small) nonlinear strength constant values of cubic and quintic orders have quantitative effects on the sizes (range value and depth value) of the existent stability range. This figure (Fig. 1) also shows the appropriateness of the approximation $U(\nu) \simeq U_0(\nu)$ [following Eq. (23) for small values of g_1 and g_2] in demonstrating the key qualitative evolution pattern of $\nu(t)$ as shown in Eq. (25).

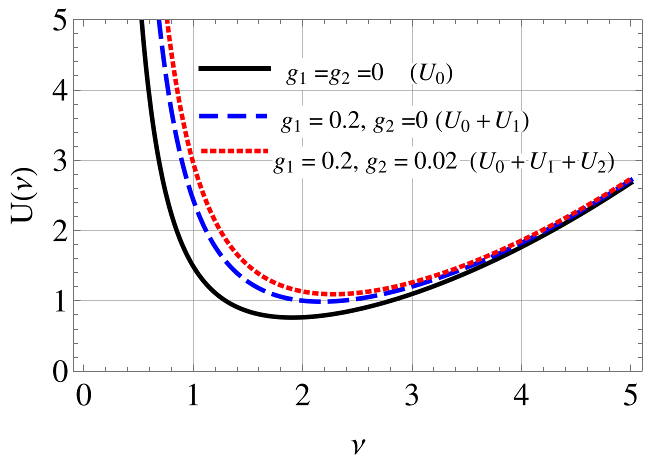

FIG. 1. The potential $U(\nu)$ vs ν incorporating different orders' nonlinearity strength constants g_1, g_2, with three typical combinations of parameters showing their impact and contribution to the stability range of the derived system distribution width $\nu(t)$ (g_1 and g_2 are in units of $\frac{4\pi\hbar^2 a_0}{m}$, and a_0 is the initial s-wave scattering length).

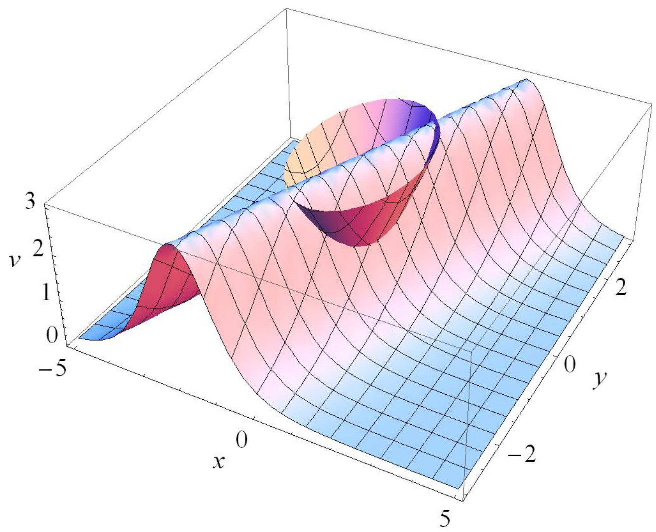

FIG. 2. c_s and v_f vs x, y in the middle timing point of the timing range where $\dot{\nu}(t) > 0$; the vertical coordinate is just the velocity value v for c_s and v_f. The intersecting curve is the sonic horizon of the two-dimensional BEC that was investigated. (Wave-like surface is the c_s distribution, and the bowl-shape surface is the v_f distribution.)

The velocity of the system is

$$v_f(x,y,t) = \frac{\hbar}{2mi}(\psi^*\nabla\psi - \psi\nabla\psi^*) = \frac{\dot{\nu}(t)}{\nu(t)}(x\vec{e_x} + y\vec{e_y}) = \frac{\dot{\nu}(t)}{\nu(t)}r\vec{e_r}. \tag{27}$$

In Sec. III, the two-dimensional wave function $\psi(x,y,t)$ determined by the self-similarity method is denoted as $\psi_s(x,y,t)$ in Eq. (8). According to Eq. (8), the system flow velocity obtained from the self-similar method is

$$v_s(x,y,t) = \frac{\hbar}{2mi}(\psi_s^*\nabla\psi_s - \psi_s\nabla\psi_s^*) = \frac{1}{2}\frac{z_t(t)}{z(t)}(x\vec{e_x} + y\vec{e_y}) = \frac{1}{2}\frac{\dot{z}(t)}{z(t)}r\vec{e_r}. \tag{28}$$

The following relation between $z(t)$ and $\nu(t)$ can be obtained by comparing Eq. (17) with Eq. (25), which takes the following form:

$$z(t) = \nu(t)^2. \tag{29}$$

Comparing Eq. (27) with Eq. (28), we can see that the velocity of BEC derived by the self-similar method in Sec. III is consistent with what we derived via the modified variational method here in this section.

V. SONIC BLACK HOLE HORIZON FORMATION FOR A TWO-DIMENSIONAL BOSE–EINSTEIN CONDENSATE WITH QUINTIC-ORDER NONLINEARITY

In recent years, an analog black hole that forms in BEC has become a hot topic for the study of black hole related problems. These problems include horizon formation dynamics, which initiates the occurrence of famous Hawking radiation in an analog black hole. Such horizon is just the sonic black hole horizon in our study. Based on the theoretical results that we derived in Secs. II–IV, we investigated a typical sonic black hole horizon formation when a two-dimensional BEC exhibits soliton evolutionary behavior. As shown in the ensuing steps, such sonic black hole horizon formation with a concrete shape in a dynamically stable manner depends on the stable motion pattern of $\nu(t)$ [and its "velocity" $\dot{\nu}(t)$] around its local minimum of "potential" $U(\nu)$ shown in the curve of Fig. 1, which is stable with respect to perturbations if the potential $U(\nu)$ curve's local minimum region is not shallow. Such a condition also makes a sonic black hole horizon shape stable. According to the sonic horizon formation criteria, the sonic horizon is the boundary between the two-dimensional BEC system flow speed's ultrasonic and subsonic region, which is a curve in a two-dimensional BEC system. To determine the location of the sonic horizon curve, we need to calculate the spatial distribution of the 2D BEC system's sound velocity c_s[32] and the system's flow velocity v_f. These two velocity quantities are calculated from the wave functions that we derived in Secs. II–IV as follows:

$$c_s = \sqrt{\frac{g_1}{m}|\psi(x,t)|} \tag{30}$$

and from Eq. (27) [or Eq. (28)]

$$v_f = \frac{\dot{\nu}(t)}{\nu(t)}r\vec{e_r}. \tag{31}$$

The sonic horizon is the two-dimensional curve satisfying the following equation:

$$v_f(x,y,t) - c_s(x,y,t) = 0. \tag{32}$$

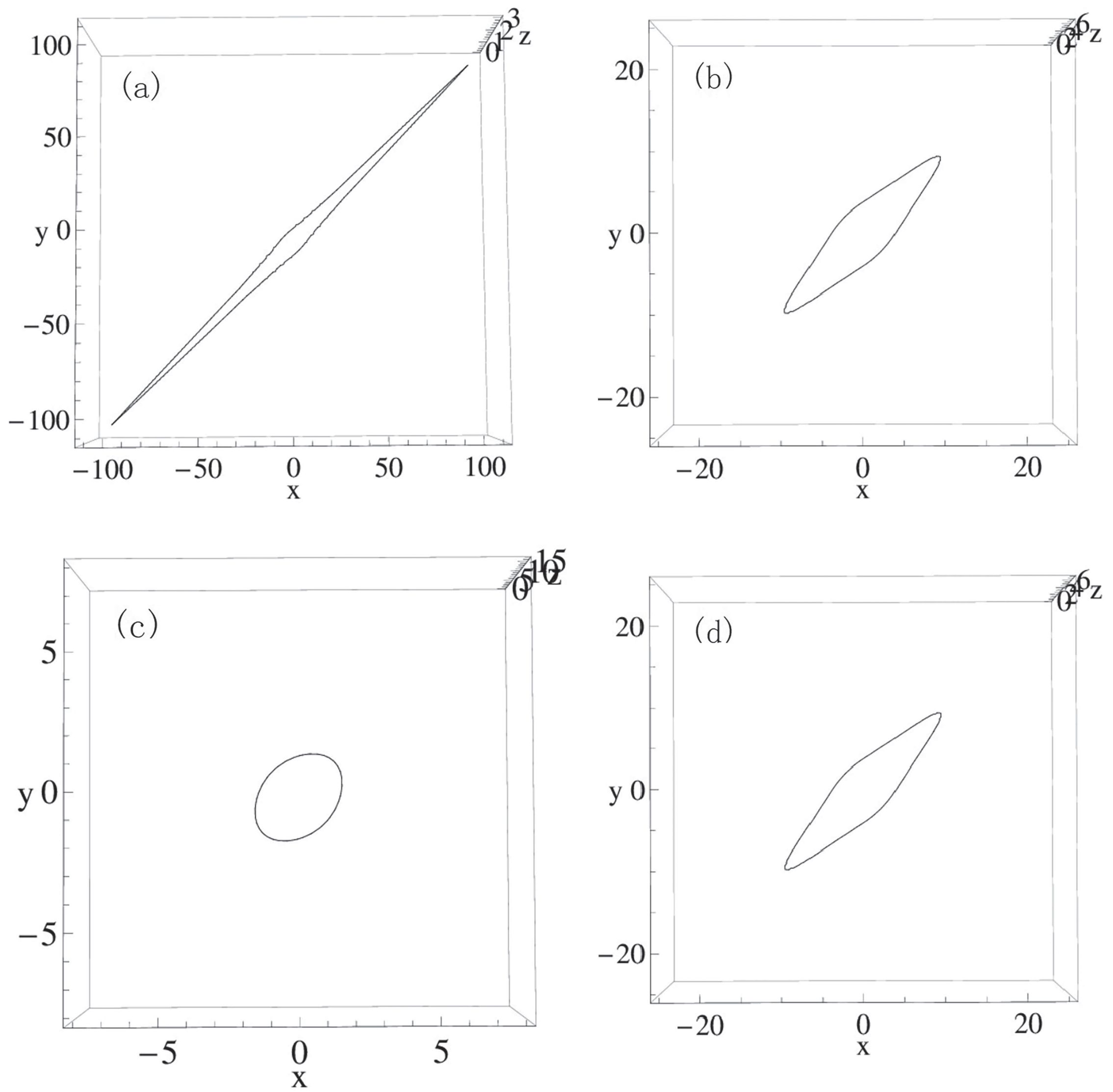

FIG. 3. The evolutionary patterns of the sonic horizon at four timing positions (a) $t = \frac{7}{12}T_0$, (b) $t = \frac{2}{3}T_0$, (c) $t = \frac{3}{4}T_0$, and (d) $t = \frac{5}{6}T_0$; this two-dimensional sonic horizon exists in the time range $[T_0/2, T_0]$ in one evolutionary period T_0. The range of the vertical z axis indicates the magnitude of the flow/sound velocity of the system at the location of the sonic horizon.

It is the intersecting curve of surface $z_1 = v_f(x, y, t)$ and $z_2 = c_s(x, y, t)$. The t dependence in Eq. (32) comes from a parametric function $\nu(t)$, which is periodic. As shown in Eq. (31), $\nu(t)$ is positive definite, with $\dot{\nu}(t)$ switching between positive and negative signs in one period of $\nu(t)$. Therefore, Eq. (32) has a solution with roughly a half-period when $\dot{\nu}(t)$ is positive. This means that the sonic horizon in our study comes into being, evolves, and periodically disappears. At the middle timing point of a period timing range, the existence of the sonic horizon is shown in Fig. 2. The location of the sonic horizon in the two-dimensional BEC is the projection of the crossing curve between surface c_s and surface v_f on the xy plane. The evolutionary patterns of the two-dimensional sonic horizon at four timing positions within one evolutionary period of the system are shown in Fig. 3. It can be seen that the sonic horizon appears as a narrow diamond strip and evolves into a quasi-circular shape and then back to a diamond shape. It then disappears and reappears in the corresponding timing position of the next oscillation period. As pointed in the prior numerical study of sonic horizon,[33] the hawking radiation in a two-dimensional setting as well as in a three-dimensional setting is related to the sonic-analog of the hawking temperature T_{pc}, which is proportional to the spatial gradient of the difference of system sound and flow velocity at the location of sonic horizon. The system in this study is isotropic in the two-dimensional study, and similar to the three-dimensional scenario in the prior work,[33] the T_{pc} is solely dependent on the radial gradient difference between the system flow and the sound velocity. The incorporation of quintic nonlinearity has quantitative distribution effects of gradients for a system flow velocity [dependent on $v(t)$ and $\dot{v}(t)$] and sound velocity (dependent on the system wave function) in the evolutionary period and may produce a noticeable T_{pc} value (a higher gradient difference but with a shorter sonic horizon existence time span) regarding the practical sonic horizon formation key feature identification. It is necessary to combine certain related physics problems for the investigation of sonic horizon radiation issues.

Our derived results also demonstrate that there is dramatic evolution of the sonic horizon during the initial formation stage and the later disappearance stage of sonic horizon formation with a relative larger spatial gradient (and larger T_{pc}) of velocity difference. This calls for experimental verification via the detection of sonic-analog of hawking radiation, especially in certain stages of the sonic horizon formation.

VI. CONCLUSION

In this study, we investigated the soliton behavior and associated sonic horizon dynamics for a two-dimensional BEC with nonlinearity up to a quintic order. Based on the two-dimensional GPE with quintic-order nonlinearity, we first derived the system's bright soliton solution via self-similar and modified variational methods. We were able to reach an identical kinematic quantity-system flow velocity through two different approaches, which corroborated the existence of bright soliton behavior for a two-dimensional system with quintic-order nonlinearity. We then analyzed the sonic horizon formation dynamics for the two-dimensional BEC system using the wave function formulation derived from the above-mentioned two distinct methods. We demonstrated the periodic occurrence and disappearance of the sonic horizon, which evolves from an initial line to a symmetrical closed curve and then its disappearance from a single line. Our theoretical results will lay a foundation for further studies of two-dimensional analog sonic black holes, such as Hawking radiation in two-dimensional quantum systems described by the GPE model. The results can also be used in future studies to guide the experimental observation of soliton behavior and an associated horizon formation phenomenon in a two-dimensional BEC with quintic-order nonlinearity.

ACKNOWLEDGMENTS

This work was supported by the National Natural Science Foundation of China (NNSFC) under Grant Nos. 11547024 and 11874185.

DATA AVAILABILITY

Data sharing is not applicable to this article as no new data were created or analyzed in this study.

REFERENCES

[1] G. I. Stegeman and M. Segev, Science **286**, 1518 (1999).
[2] M. Shen, H. Ding, Q. Kong, L. Ruan, S. Pang, J. Shi, and Q. Wang, Phys. Rev. A **82**, 043815 (2010).
[3] N. J. Zabusky and M. D. Kruskal, Phys. Rev. Lett. **15**, 240 (1965).
[4] Y. S. Kivshar and B. Luther-Davies, Phys. Rep. **298**, 81 (1998).
[5] G. P. Agrawal, *Nonlinear Fiber Optics* (Academic, San Diego, 2007).
[6] S.K. Liu, Z.T. Fu, Z. G. Wang, and S. D. Liu, Commun. Theor. Phys. **49**(5), 1155–1158 (2008).
[7] S. K. Adhikari, Phys. Rev. A **63**, 043611 (2001).
[8] S. K. Adhikari and L. Salasnich, Phys. Rev. A **78**, 043616 (2008).
[9] A. X. Zhang and J. K. Xue, Chin. Phys. Lett. **25**, 39 (2008).
[10] H. Liu, D. H. He, S. Y. Lou, and X. T. He, Chin. Phys. Lett. **26**, 120308 (2009).
[11] S. Zhang, J. M. Ba, Y. N. Sun, and L. Dong, Z. Naturforsch. **64a**, 691–696 (2009).
[12] J. X. Fei and C. L. Zheng, Chinese J. Phys **51**(2), 200 (2013).
[13] Z. Y. Yan and V. V. Konotop, Phys. Rev. E **80**, 036607 (2009).
[14] F. J. Yu, Appl. Math. Comput. **219**, 5779–5786 (2013).
[15] Y. V. Kartashov, G. E. Astrakharchik, B. A. Malomed, and L. Torner, Nat. Rev. Phys. **1**, 185 (2019).
[16] B. A. Malomed, Eur. Phys. J. Spec. Top. **225**, 2507–2532 (2016).
[17] C. Trallero-Ginera, J. C. Drake-Pereza, V. Lopez-Richardb, and J. L. Birmanc, Physica D **237**, 2342 (2008).
[18] R. Atre, P. K. Panigrahi, and G. S. Agarwal, Phys. Rev. E **73**, 056611 (2006).
[19] Y. S. Cheng, H. Li, and R. Z. Gong, Chin. Opt. Lett **3**, 715–718 (2005).
[20] H. Li and D. N. Wang, Chin. Opt. Lett. **6**, 611–614 (2008).
[21] A. V. Prokhorov, M. G. Gladush, M. Y. Gubin, A. Y. Leksin, and S. M. Arakelian, Eur. Phys. J. D **68**, 158 (2014).
[22] W. G. Unruh, Phys. Rev. Lett. **46**, 1351 (1981).
[23] L. J. Garay, J. R. Anglin, J. I. Cirac, and P. Zoller, Phys. Rev. Lett. **85**, 4643 (2000).
[24] A. X. Zhang and J. K. Xue, Chin. Phys. Lett. **25**, 39 (2008).
[25] H. Liu, D. H. He, S. Y. Lou, and X. T. He, Chin. Phys. Lett. **26**, 120308 (2009).
[26] T. H. Johnson, M. Bruderer, Y. Cai, S. R. Clark, W. Bao, and D. Jaksch, Europhys. Lett. **98**, 26001 (2012).
[27] Y. Wang, Y. Zhou, and S. Y. Zhou, Sci. Rep. **6**, 38512 (2016).
[28] Y. Wang, Q. Cheng, J. Y. Guo, and W. Wang, AIP Adv. **9**, 075206 (2019).
[29] S. Cowan, R. H. Enns, S. S. Rangnekar, and S. S. Sanghera, Can. J. Phys. **64**, 311 (1986).
[30] K. I. Pushkarov, D. I. Pushkarov, and I. V. Tomov, Opt. Quantum Electron. **11**, 471 (1979).
[31] J. Yang, *Nonlinear Waves in Integrable and Non-integrable Systems* (SIAM, Philadelphia, 2010), p. 168.
[32] E. Zaremba, Phys. Rev. A **57**, 518 (1998).
[33] Y. Kurita and T. Morinari, Phys. Rev. A **76**, 053603 (2007).